Front. Earth Sci. 2019, 13(3): 596–613
https://doi.org/10.1007/s11707-018-0689-9

RESEARCH ARTICLE

The barrier river reach identification and classification in the Middle Yangtze River

Jinwu TANG[1], Chunyan HU[1], Xingying YOU (✉)[2,3], Yunping YANG[4], Xiaofeng ZHANG[3], Jinyun DENG[3], Meng CHEN[2]

1 Changjiang Institute of Survey Planning Design and Research, Wuhan 430010, China
2 Hubei Institute of Survey & Design for Water Resources & Water Power Engineering, Wuhan 430064, China
3 State Key Laboratory of Water Resource and Hydropower Engineering Science, Wuhan University, Wuhan 430072, China
4 Key Laboratory of Engineering Sediment, Tianjin Research Institute for Water Transport Engineering, Ministry of Transport, Tianjin 300456, China

Abstract Adjustments of upstream river regimes are one of the main factors affecting downstream fluvial processes. However, not all adjustments of river regimes will propagate downstream. There are some distinctive river reaches where upstream and downstream adjustments have no relevance. However, the irrelevance is neither caused by different river types nor by the different conditions of water and sediment; but rather, the channel boundaries and riverbed morphologies block the propagation effect. These are referred to here as the barrier river reach phenomena. The migration of the thalweg line is the essential reason for causing the propagation effect. Numerous influencing factors for thalweg migration exist, including 1) the average flow rate above the critical bankfull discharge, the average flow rate below the critical bankfull discharge, and their ratio, 2) the ratio of the duration of the aforementioned two periods, 3) the thalweg displacement at the entrance of the river reach, 4) the deflecting flow intensity of the node, 5) the ratio of the river width to water depth, 6) the relative width of the floodplain, and 7) the Shields number. In this study, the correlativity between the measured distances and the restricting indicators of thalweg migration in the Middle Yangtze River over the years was established. The barrier degree of 27 single-thread river reaches was subsequently assessed. These reaches included 4 barrier river reaches; 5 transitional reaches transforming from barrier to non-barrier; 10 transitional reaches transforming from non-barrier to barrier; and 8 non-barrier river reaches. Barrier river reaches were found to be important for maintaining the stability of the river regime and the transverse equilibrium of sediment transport in the downstream reaches. To some extent, the barrier river reaches may protect the natural dynamical properties from being destroyed by artificial river regulation works. Thus, they are of great significance for river management.

Keywords the barrier river reach, Yangtze River, channel adjustment, thalweg migration, identification and classification

1 Introduction

The classification and discrimination of river patterns are basic challenges in fluvial geomorphology. For example, Leopold and Wolman (1957) divided river patterns into braided rivers and meandering rivers according to the relationship between the channel gradient and the flow rate, Schumm and Khan (1971) proposed straight rivers according to the differences in the sinuosity and channel gradient, and Rust (1977) proposed anastomosed rivers according to the differences in the braiding index and sinuosity (Nanson and Croke, 1992; Nanson et al., 2010). In addition, some scholars distinguished river patterns by using the sediment transport rate, the energy consumption rate (Ferguson, 1981), and so forth. The Middle Yangtze River (hereafter, MRYR) in China shows distinct characteristics; namely, the central islands are decreasing in number yet the morphologies of the islands are relatively stable. Moreover, the river width and the size of the interfluve are smaller than those of the anastomosed rivers with similar degrees of runoff. The anabranched portions of the MRYR can be defined as bifurcated rivers (Qian et al., 1987). Different bifurcated river reaches are often connected by either meandering or straight rivers,

Received August 16, 2016; accepted November 12, 2017

E-mail: you_tang@foxmail.com

characterized by a single-thread channel. As a result, the middle-lower Yangtze River is characterized by staggered distributions of both bifurcated and single-thread river reaches (Qian et al., 1987; Wang and Yin, 2000; Wang, 2003).

The natural alluvial channel was in a constant state of adjustment in regard to scouring and siltation (Gilbert and Dutton, 1877; Davis, 1899). As long as the rates of scouring and erosion were unchanged, the states of balance between the opposing forces, such that they operate at equal rates and their effects cancel each other, would be maintained (Hack, 1960). However, after a disturbance occurs in an unconfined river channel with no restriction on either side, the channel may migrate as a whole and the river pattern may be transformed. When a disturbance destroys the transverse equilibrium of sediment transport in a confined channel, the river pattern can't change due to the constraint of the channel boundary. The river channel, however, will be adjusted by the changes in the location and direction of the flow dynamic axis (i.e., the connection line of the maximum vertically averaged flow velocity point of each cross-section, also called the main stream line). These changes in effect absorb the influence of the disturbance and help restore the transverse sediment transport balance. This process is referred to in this paper as river regime adjustment. Obviously, when the channel is adjusted to a transverse sediment transport equilibrium state, the planar position of the flow dynamic axis and the planar morphology of the point bars and pools can be maintained for a certain period of time, during which the river regime can be considered stable (Han, 2011; Lobera et al., 2015; You et al., 2017a).

The causes of river regime adjustments include artificial disturbances, such as dam construction (Henshaw et al., 2013), bridge construction, sand mining (Armaş et al., 2013), dredging, and canalization (Hajdukiewicz et al., 2016). Additionally, river regime adjustments could be caused by natural disturbances, such as changes in the channel boundary condition (Ramos and Gracia, 2012) or water and sediment conditions, bank collapse (Xia et al., 2014), neck cut-offs (Cserkész-Nagy et al., 2010), chute cut-offs (van Dijk et al., 2014), geological tectonic movements (Roy and Sahu, 2015), or climate change (Wolman and Gerson, 1978). A river regime adjustment may threaten flood safety, obstruct navigation, or harm aquatic and riparian ecosystems. Therefore, establishing management practices to minimize these disturbances and maintain the river regime stability has become the primary focus of fluvial geomorphologists.

Studies (Huang and Liu, 1991; Schuurman et al., 2016a) have shown that the wave of the flow dynamic axis was the carrier of the energy of water flow. It was the motive force of the generation and propagation of the upstream and downstream effect. River regime adjustments caused by disturbances would propagate downstream, and thus affect long reaches downstream (Goodbred and Kuehl, 1998). The upstream sustained dynamic perturbation caused by sustained meander migration (Zolezzi and Güneralp, 2016), as well as sustained downstream migration of point bars and pools (Xu and Bai, 2013), similar to a propagating wave (van Dijk et al., 2013). Although the river bends could migrate both upstream and downstream simultaneously (Cserkész-Nagy et al., 2010), the effects of upstream disturbances were minor and only occurred through the backwater effect, i.e., the geomorphic instability caused by disturbances was primarily amplified in the downstream direction (Schuurman et al., 2016b). A study on the long-term and long-flow-path channel evolution in the MRYR (Jun et al., 2012) showed that upstream river regime adjustments could lead to downstream chain reactions involving thalweg migration, deposition or erosion of central islands, river bank collapses, and translocations between the main branches and secondary branches. Considering the randomness and inevitability of artificial disturbances, this paper primarily evaluated the propensity of river regime adjustments to transfer downstream.

During the propagation process whereby the upstream river regime adjustments transfer downstream, some special river reaches may block the transfer effects. This is referred to as the barrier river reach phenomenon in this study. The natural properties of such river reaches may alleviate some of the adverse effects of upstream river regime adjustments on downstream reaches, thus mitigating the influence of artificial river regulation works on the channel's natural dynamic balance. Fryirs et al. (2007) introduced the concept of landform impediments, termed buffers, barriers, and blankets, which could limit the geomorphic connectivity and disrupt longitudinal linkages. Reid and Brierley (2015) weighed the downstream sensitivities by evaluating the 'freedom space to move' or 'capacity for adjustment'. For a channel where both sides were confined and therefore did not have 'freedom space to move', the migration range of the thalweg line could be used as an indicator to assess the barrier strength. A summarization and analysis of a large number of phenomena in the MRYR (You et al., 2016) have shown that some river reaches could maintain the morphological stability of the riverbed and the singleness of the main channel, thereby weakening or eliminating the influence of upstream river regime adjustments on the downstream river reaches. The discovery of such river reaches is of great importance for river management and maintenance. Because of the stable channel boundary conditions, the barrier river reach can sustain the transverse equilibrium of sediment transport as long as no artificial disturbances destroy the boundary conditions, no matter the variation of water and sediment conditions or the adjustments caused by artificial or natural disturbances, which is conducive to the stability of the downstream river regime (You et al., 2017b).

Studies have shown that different channel patterns can have different sensitivities and abilities to cope with fluvial geomorphic change (Downs and Gregory, 1993). After the upstream river regime adjusts, a straight river reach can change the position of the thalweg transition by moving the point bar (van Dijk et al., 2013). A meandering river can react to the sustained migration of the thalweg line by bank erosion and bar growth or floodplain accretion (van Dijk et al., 2013; Schuurman et al., 2016b). Furthermore, a bifurcated river can propagate the instability in the downstream direction by means of alterations in the water and sediment divisions at different bifurcation locations (Schumm, 1985; Schuurman et al., 2016a). A straight or meandering river with a single-thread channel is relatively narrow and deep with low riverbed mobility, and the main stream lines are usually stable (David et al., 2016). A bifurcated river has multiple-thread channels, which are relatively wide and shallow, and the main stream line is prone to translocate between the two branches (Campana et al., 2014). Because the adjustment of the multiple-thread channels is more sensitive than the single-thread channel, the functions on restricting the migration of the main stream line and reducing the channel deformation are bound to exist in the single-thread channel. Considering the characteristic of staggered distribution of straight and bifurcated channels in the MRYR (Chen et al., 2012; Song et al., 2016), it would be interesting to investigate whether the downstream single-thread river reaches propagate the upstream adjustments or whether they block this propagation effect. This has an important influence on the long-flow-path stability of the river regime.

In this paper, 27 single-thread river reaches in the MRYR were investigated, through analyzing the channel evolutive characteristics and the river regime adjustments regularities, the concept of the barrier river reach was identified. By analyzing the measured data, the influencing factors for thalweg migration were summarized. Additionally, the strength of the channel boundary restricting on the thalweg migration was studied. By establishing the empirical relationships between the measured distances and the restricting indicators of the thalweg migration, the barrier properties could be classified into four types.

2 Study area

The Yangtze River is the largest river in China, with a total length of more than 6300 km. The Yichang to Hukou Reach, with a total length of 1893 km, is named as the MRYR. The riverbed from Shashi to Hukou is sandy. At the south bank of the MRYR, there are three outlets, namely, Songzi, Taiping, and Ouchi, which divert water and sediment into Dongting Lake. These waters then return to the Yangzte River at the confluence of Chenglingji after being stored and dispatched. Hanjiang River and Poyang Lake converge into the Yangtze River at Wuhan and Hukou, respectively. The Shashi–Chenglingji Reach, Chenglingji–Wuhan Reach, and Wuhan–Hukou Reach are monitored by the Jianli, Luoshan, and Hankou hydrological stations, respectively. The specific locations of these areas and hydrological stations have been marked in Figs. 1(a)–1(c), illustrating the daily averaged flow and sediment concentration processes of each hydrological station from 1955–2013. The longitudinal channel profile is also shown in Fig. 1(d). The current river adjustment patterns include bank collapses, bend abandonment and point bar cutting, neck cut-offs, substantial erosion or deposition of the point bar and central bar, and translocations between the main branch and secondary branch. Their common characteristic is the drastic migration of the thalweg line.

Because of the high mobility of the sandy riverbeds (Zhang et al., 2017), adjustments in the river regime in the MRYR display obvious characteristics of downstream propagation. Qian et al. (1987) stated, “If one bend changes, every downstream bend changes.” This propagation effect usually lasts for years or even decades and often involves multiple river reaches. Owing to the large number of embankments and revetments built since the construction of new China, the erosion resistance of the channel boundary has been significantly enhanced. A narrow groove configuration was gradually formed when the channel cut down which is beneficial for restricting the thalweg migration and shaping the barrier river reach. The focus of this paper was based on the research of 27 single-thread river reaches in the Shashi–Hukou Reach, as shown in Fig. 1. The remote sensing images are compiled according to Landsat satellite data products. Due to the characteristics of the staggered distributions of different river types, each shorter single-thread river and bifurcated river is carefully divided, ensuring each dynamic adjustment mechanism is maintained, as shown in Fig. 1.

3 The propagation and barrier phenomenon

At the position of the main stream line, the flow velocity is large, the sediment-carrying capacity is strong, and the riverbed erosion is significant. Alternatively, at locations far away from the main stream line, the flow velocity is small, the sediment-carrying capacity is weak, and the riverbed is silting up. The long-term erosion of water flow contributes to the fluvial geomorphology like the thalweg or the main channel. With an increase in flow, the main stream line separates from the original thalweg, diffuses onto the floodplain, and even diverts into new areas trying to shape a new thalweg. Within one hydrological year, the flow rate level change exacerbates the fluctuation of the main stream line. After the cumulative effect of several hydrological years, the old thalweg withers away and the

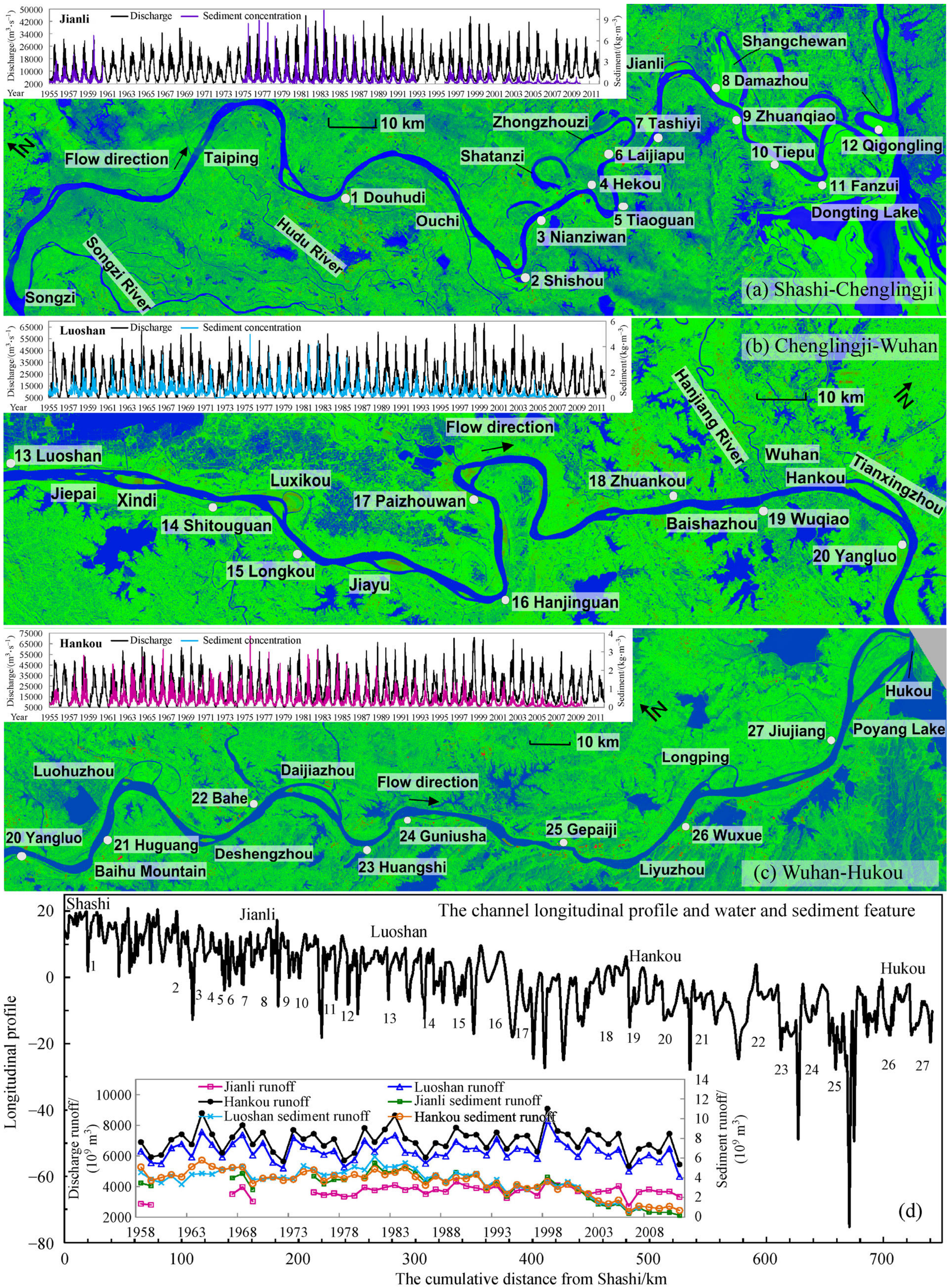

Fig. 1 Sketch map of river channel and hydrological situation. (a) Shashi–Chenglingji Reach; (b) Chenglingji–Wuhan Reach; (c) Wuhan–Hukou Reach; (d) Flow and sediment concentration and longitudinal profile.

new thalweg becomes more pronounced. Ultimately, the exhaustive translocation occurs, accompanied by the drastic adjustments of riverbed morphology. Therefore, the propagation and barrier phenomena of the river regime adjustments can be reflected through the thalweg migration and the corresponding riverbed deformation over time.

3.1 The sketch map of a barrier river reach

Typically two natural stimuli cause downstream propagation of channel adjustment. One is the modification of flow and sediment condition, the other is the thalweg migration caused by the upstream river regime adjustment. This paper focuses on the latter. Visibly, the adjustment of the upstream river regime provides an initial disturbance for the downstream entrance. In some reaches with poor erosion resistance of river bank or sandbar margin, the thalweg may magnify its migration space through collapsing and broadening the channel boundary. The thalweg displacement at the entrance could then be amplified in the downstream reaches. However, in some reaches, the disturbance effects may be reduced or eliminated, which is conducive for maintaining the stability of the river regime. Thus, not all river regime adjustments will be transferred downstream. As long as there are no artificial disturbances to destroy the boundary conditions due to strong anti-interference capacities, some river reaches can maintain the lateral equilibrium of sediment transport and resist the thalweg migration caused by the upstream channel adjustments. They can stabilize their morphologies of point bars and pools, thereby preventing the upstream river regime adjustments from propagating downstream. These types of river reaches can be defined as barrier river reaches.

The Longkou Reach is an illustration of a barrier river reach. As shown in Fig. 2, this reach connects upstream with the Luxikou Reach, and downstream with the Jiayu Reach, which are both bifurcated rivers. Based on many measured data over the years, the interannual periodic evolution of the Luxikou Reach can be described as follows: the low bar at the head of the middle bar was cut and a new middle channel was generated → the new middle channel developed and moved downstream → the new middle channel combined with old channels → the middle channel continued bending and moved downstream → the new middle channel regenerated and developed. There have been five evolutive cycles since the 1930s: 1935–1958, 1959–1970, 1971–1982, 1983–2005, and 2006–present. Jiayu Reach also displayed interannual periodic evolution. In each cycle, the Wangjiazhou point bar was deposited and expanded, and then eroded, moving downstream and ultimately joining with the Fuxing bar. Meanwhile the north branch transformed from a single-groove to a double-groove and then to a single-groove again. Since the early 1920s, Jiayu Reach has experienced two evolutive cycles: 1933–1980 and 1980–present. A comparison of the interannual evolution of Jiayu Reach and Luxikou Reach shows that, even though both evolutions were periodic, they had a different number of cycles, and the initial times of their cycles were not synchronized and were not caused by the retardation of the downstream river reach. The modes of the river channel deformations were also different. The thalweg in the Luxikou Reach alternately migrated between the two branches, but the thalweg in the Jiayu Reach migrated in the north branch interior. It is evident that Longkou Reach

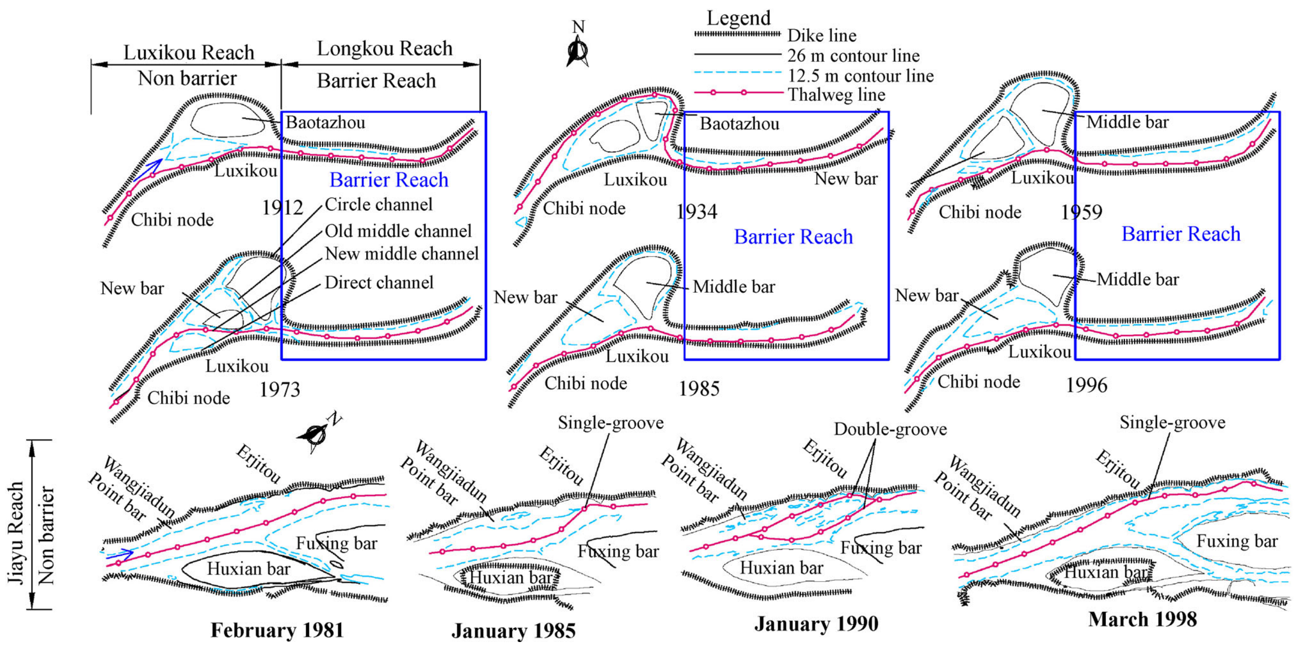

Fig. 2 Sketch map of the Barrier River Reach.

prevented the propagation of river regime adjustment from Luxikou Reach to Jiayu Reach. Moreover, the channel morphology and thalweg position of Longkou Reach remained unchanged regardless of the evolutive cycle stage of Luxikou Reach, thereby providing a stable outflow direction for Jiayu. This meant that Longkou Reach exerted the role of a barrier.

3.2 The propagation penomenon of river regime adjustment

The phenomenon of the downstream propagation of river regime adjustment is illustrated as follows. The Wuhan Reach was divided into: the Baisha bar bifurcated Reach (from Zhuankou to Nianyutao), the Wuqiao single-thread Reach (from Nianyutao to Xujiapeng), and the Tianxing bar Reach (from Xujiapeng to Yangluo). As shown in Fig. 3, during the mid- to late 19th century, the thalweg of the Baisha bar Reach inclined to the south bank, then to Hankou on the north bank due to the deflecting flow effect of the Snake node, and then entered the north branch of the Tianxing bar Reach, thereby becoming the main branch. By the mid-20th century, the thalweg of the Baisha bar Reach moved north, and the Baisha bar and Qian bar were generated near the south bank. A deflecting flow from the Turtle node on the north bank forced the thalweg to Wuchang on the south bank and then entered the south branch of the Tianxing bar Reach, which thus developed into the main branch. Comparing these two evolutive processes, the planar positions of the upstream and downstream thalwegs were changing synchronously and correspondingly. Obviously, it was the north shift of the thalweg in the Baisha bar Reach that changed the planar position of the thalweg at the entrance of the downstream reach, making the south branch of Tianxing bar the main channel and consequently, the river regime adjustment transferred downstream from Baisha bar to Tianxing bar.

3.3 The barrier phenomenon of river regime adjustment

The non-synchronization of the river regime adjustment from upstream to downstream in the barrier river reach is not caused by different conditions of water and sediment. As shown in Fig. 4, the Huangshi Reach connects upstream with the Daijia bar bifurcated Reach, and downstream with the Guniusha single-thread Reach. The Daijia bar Reach showed a tendency of alternating translocation between the circular channel and the direct channel: the thalweg located in the circular channel in 1958 and 1964, shifted to the direct channel in 1977 and 1997, with a brief migration to the circular channel in 1987, and in 2003, translocated to the circular channel. However, the migrations of the thalweg of Guniusha Reach were closely related to the erosion and deposition of the Guniusha point bar. When the Guniusha point bar deposited and expanded, the thalweg turned north in 1959, 1977, and 1987. When the Guniusha point bar scoured and shrunk, the thalweg turned south in 1965, 2000, and 2003. In the same year, the processes of water and sediment in the adjacent river reaches were nearly the same, but the evolutive regularities of Daijiazhou and Guniusha Reaches were different. Obviously the Huangshi Reach in the midstream, with a long-term stable channel morphology, prevented the upstream river regime adjustment from transferring downstream, resulting in a smaller migration amplitude of the thalweg in the downstream reach than in the upstream reach. Alternatively, if the river reach in the midstream does not have the barrier effect, the upstream and downstream river regime adjustments will have synchronous correspondence, which can be confirmed from the examples in the preceding section. Therefore, making full use of the natural advantage of barrier river reaches is beneficial for maintaining the stability of long-term and long-flow-path river regime, dispensing with the constant water and sediment conditions.

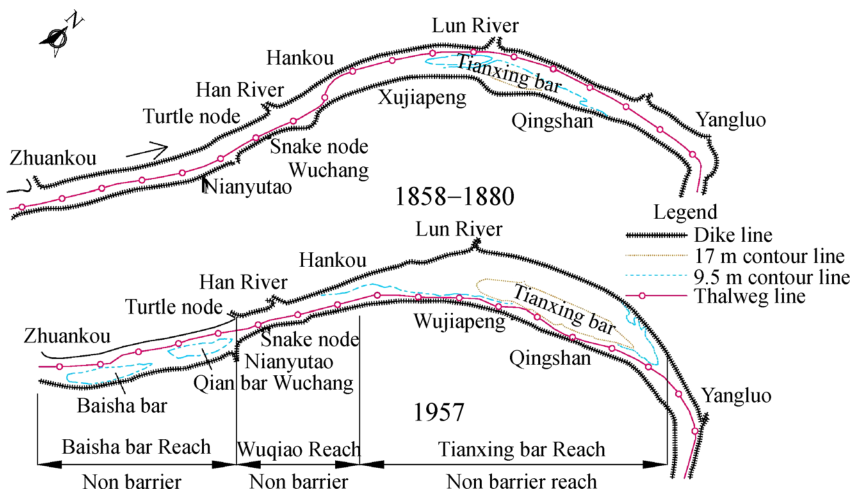

Fig. 3 Diagram of the river regime propagations in the Baisha bar–Tianxing bar Reach.

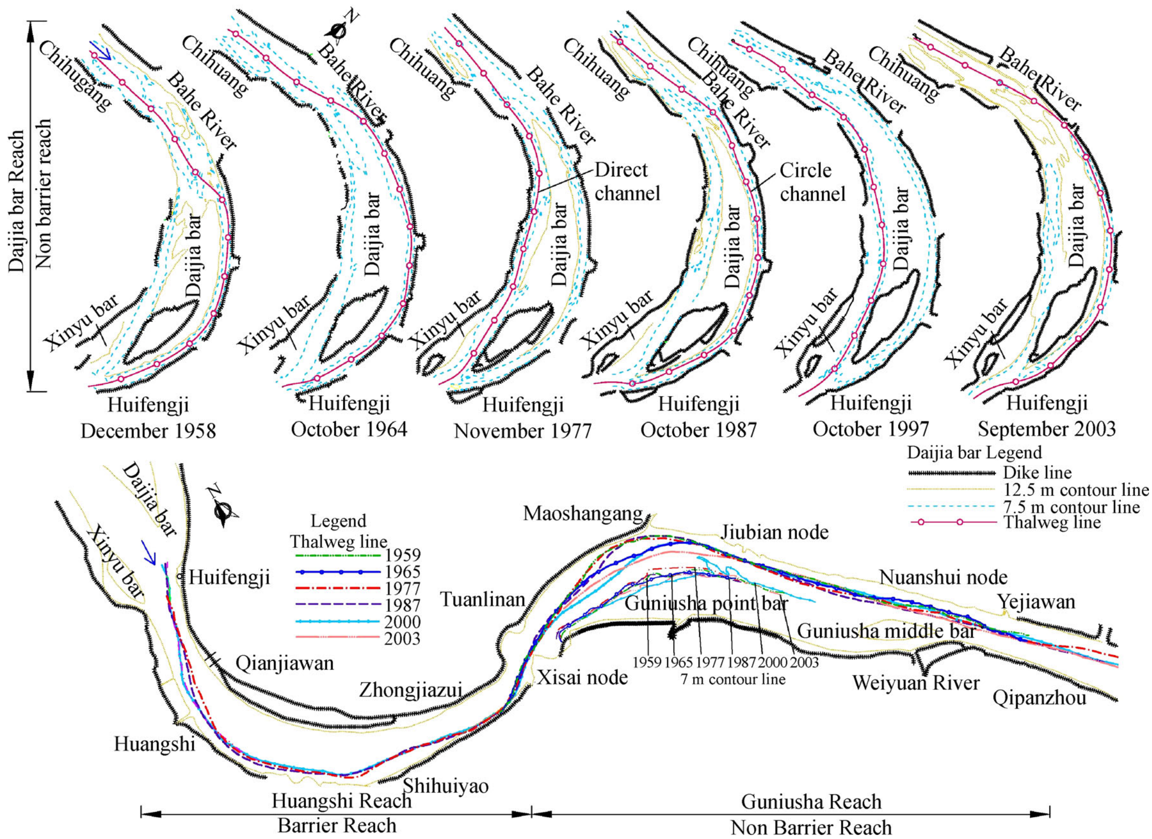

Fig. 4 Diagram of the river regime barriers in the Daijia bar–Guniusha Reach.

The inconsistency of upstream and downstream river regime adjustments from the barrier river reach is not caused by the different river types. Although the dynamic adjustment mechanism of the same river type is typically uniform, some evolutive phenomena appear to display inconsistent characteristics. As shown in the right section of Fig. 5, the upstream and downstream reaches of the Zhuanqiao Reach are separately composed by the Damazhou Reach and Tiepu Reach, both of which are defined as single-thread straight rivers. The thalweg position of Damazhou is mainly affected by the river regime of the upstream Jianli Reach. When the turtle bar connected with the Xinhekou point bar in the right bank as a whole, the thalweg of Damazhou moved downward in the middle, as occurred in 1966, 1973, and 1987. When the turtle bar was cut and the central bar at the head of the turtle bar was relatively large in scale, the thalweg of Damazhou moved downward along the west bank, as in 1973. When the central bar at the head of the turtle bar was relatively small in scale, the thalweg of Damazhou moved downward along the east bank, as in 1993. It can be seen that even though the upstream and downstream reaches were of the same river pattern, they still appeared as different evolutive regularities because the barrier river reach in the midstream blocked the flow-topographical dynamic connectivity. In general, the evolutive regularities of the river regime between the upstream and downstream of the barrier river reach were not synchronous or correlated, nor were they caused by the different water-sediment conditions or the flow-topography dynamic nonuniformity of different river types. It is the barrier river reach itself blocking the flow-topography dynamic connectivity among upstream and downstream.

Given a disturbance at the entrance of continuous curves, the downstream curves may appear as a continuous bending and downstream migration (Schumm, 1985). However, this chain deformation is also conditional. When there are barrier river reaches among the continuous curves, the chain reaction may be interrupted. The left section of Fig. 5 shows the Nianziwan-Tashiyi Reach with continuous curves, where the Nianziwan, Shantanzi, Zhongzhouzi curves were naturally or artificially cut-off in 1949, 1972, and 1967, respectively. After the Nianziwan cut-off, the top curve of Huangjiaguai migrated downstream, drastically collapsing the bank at the entrance of Shatanzi Reach and the main channel east-convex. After the Shatanzi cut-off, the channel downstream from the outlet of the diversion canal evolved from west-convex to east-convex, with a long river bank collapse upstream from Tiaoguan. However, this phenomenon did not cause channel deformation downstream from Tiaoguan. Furthermore, after the Zhongzhouzi cut-off, the bank downstream

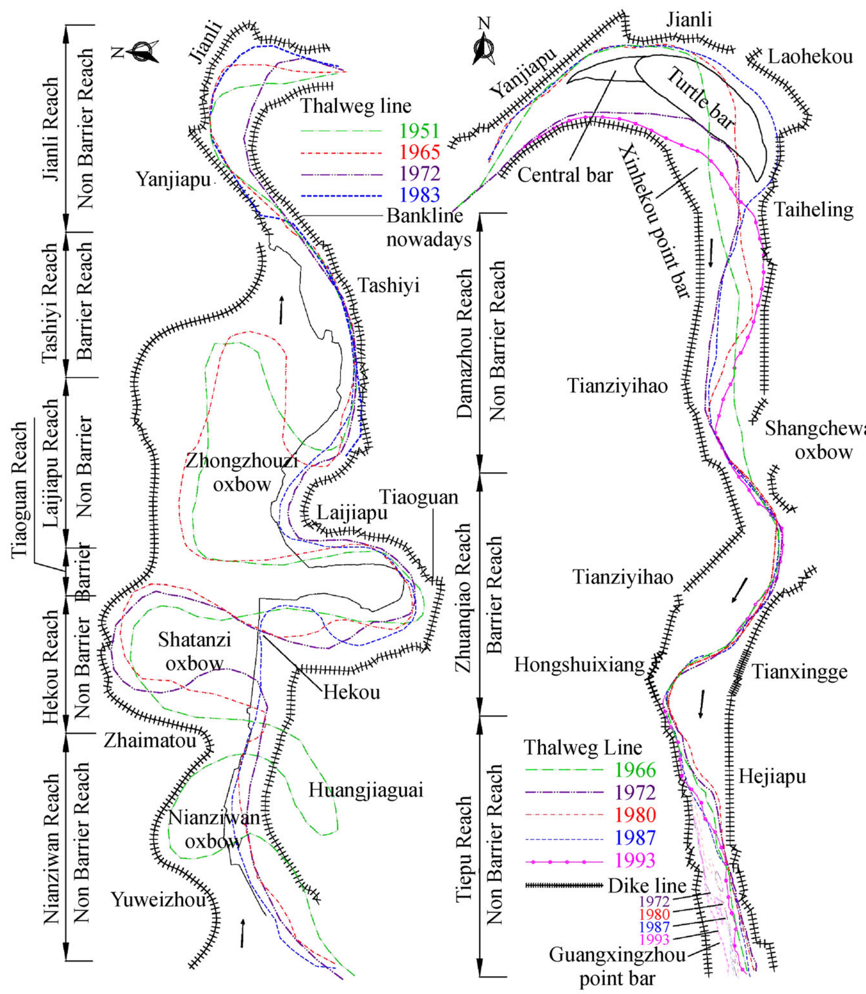

Fig. 5 Diagram of the river regime barriers in the Nianziwan–Tiepu Reach.

from the diversion canal outlet rapidly retreated 1.5 km, but the Tashiyi Reach downstream showed no significant deformation. It can be seen that the morphologies of Tiaoguan and Tashiyi remained stable, weakening the chain reaction of the upstream cut-off on the downstream channel evolution and preventing the upstream river regime adjustment from propagating downstream.

4 Methods and data

4.1 Methods

The above analysis illustrates the definition of the barrier river reach, but the best process to identify and classify them is still a question. Some hydromorphological parameters may be useful to discriminate the basic characteristics of different reaches, such as ‘width to depth ratio’, ‘unit stream power’, and ‘Shields number’. The wandering index, introduced by Qian et al. (1987), incorporated the relative speed of the rise in the flood peak, the relative fluctuation amplitude of flow in the flood season, the relative mobility of riverbed material, the relative width of the river floodplain, and the ratio of width: depth. Given that, a barrier river reach enables itself to resist the change of the position and direction of the thalweg caused by upstream river regime adjustments, and stabilizes the thalweg position in the downstream reaches. Therefore, by analyzing the migration amplitude of the thalweg at the entrance of the river reach caused by adjustments of the upstream river regime and by studying the ability of the river reach to restrict this fluctuation, one can classify the barrier degree. This paper used the model of Qian et al. (1987)for reference and established relationships between the measured distance and the restricting indicators of the thalweg migration to identify and classify the barrier properties in different river reaches.

First, the change of flow rate is a driving force for thalweg migration (Xia et al., 2016; Zhang et al., 2017). If the flow level is different, the sinuosity of the flow dynamic axis line will change. The flow dynamic axis line straightens during the flood period, but curves in the dry season. Qian et al. (1987) described thalweg migration as taking place via gradual changes and mutations, whereby the gradual changes refer to the flow-path changes caused by the different flow rates and different inertial forces, the mutations refer to the sudden steering towards the new thalweg and the abandonment of the original thalweg, which is rapidly deposited as a result of abrupt decreases in the sediment carrying capacity after a flood. In a hydrological year, after the flow rate increases and exceeds the critical bankfull discharge (i.e., the flow level corresponding to the water level equal to the crest elevation of the floodplain), the main stream line separates from the original thalweg and diffuses to other grooves on the floodplain. When the water level drops again, the main stream line returns to the original thalweg because new grooves have not yet burst through and a new thalweg has not yet developed. After the cumulative effect of several hydrological years, the thalweg eventually changes. It is thus evident that the larger average flows above the critical bankfull discharge are more beneficial for the gradual development of a new thalweg. The smaller average flows below the critical bankfull discharge are more conducive to abrupt bursting for a new thalweg. Thus, the $Q_{<\text{floodplain}}/Q_{>\text{floodplain}}$ can be used to characterize the effects of flow processes during two measurement times. In addition, the duration of the flow process also affects the thalweg migration. Specifically, the longer cumulative days above the critical bankfull discharge are more favorable for the gradual shift of the thalweg. On the other hand, the shorter numbers of cumulative days below the critical bankfull discharge are more favorable for a sudden shift of the thalweg. Therefore, the $T_{<\text{floodplain}}/T_{>\text{floodplain}}$ can be used to represent the effect of the flow duration.

Second, the thalweg displacement at the entrance of a river reach caused by upstream river regime adjustments is the direct cause of the downstream thalweg migration. The relationship between the migration distance of the internal thalweg and the displacement of the thalweg at the entrance of the river reach is directly proportional. The $\delta = \frac{B_{\text{bankfull}} - \delta_{\text{entrance thalweg}}}{B_{\text{bankfull}}}$ can be used as a representation of this disturbance. For a river reach with a node at the entrance of the river reach, with the upstream incoming flow direction changes, the outflow direction of the node also changes. The deflecting flow strength of the node increases with increases of the incoming flow exerting on the node. The deflecting flow strength of the node is also proportional to the relative length of the node protruding from the river bank. The deflecting flow coefficient $\lambda = \frac{B_{\text{bankful}} - L_{\text{node}}}{B_{\text{bankful}}}$ can be used as the exponent for the flow item.

Once again, the channel cross-sectional topography has a significant influence on the transverse distribution of the vertically averaged velocity (Qian et al., 1987), which affects the planar position of the main stream line. The height difference between the point bar and pool can represent the difficulty the main stream line has in diffusing over the floodplain. The smaller the height difference, the smaller the earthwork volume taken away by the water when it erodes the same width, and the shorter the time required. Moreover, the anti-scouring property of the river bank is weaker, and therefore, this is more conducive for the main stream line to migrate. The reciprocal of the ratio of width to depth (h/B) is used to represent the constraint function of cross-sectional topography. In addition, the river width is a key factor affecting the channel evolution. Wider floodplains are associated with wider migration spaces for the main stream line, and this will lead to more flow-paths after the main stream diffuses over the floodplain.

Additionally, only the narrow and deep cross-sections can restrict the migration of the main stream line (Nanson et al., 2010). Thus, the ratio of the bankfull river width to the greatest river width over the years ($B/B_{\max}$) can be used to represent the constraint effect of the floodplain on the migration of the main stream. Finally, the riverbed with greater mobility is more conducive to a lateral shift. The Shields number hJ/d_{50} characterizes the riverbed mobility, and thus, the restricting indicators for the thalweg migration can be established as follows:

$$\Theta = \left[\left(\delta \cdot \left(\frac{Q_{<\text{floodplain}}}{Q_{>\text{floodplain}}}\right)^{0.3} \cdot \left(\frac{T_{<\text{floodplain}}}{T_{>\text{floodplain}}}\right)^{0.05}\right)^{\lambda}\right]^{a} \cdot \left[\left(\frac{B}{B_{\max}}\right)^{0.6} \cdot \left(\frac{h}{B}\right)^{0.05} \cdot \left(\frac{d_{50}}{hJ}\right)^{0.1}\right]^{b}. \quad (1)$$

As shown in Eq. (1), the influencing factors of Θ can be divided into two parts. The former represents the migration intensity of the thalweg caused by the flow change or the adjustment of the upstream river regime, with a as the exponent; the latter represents the restricting effect of the channel boundary on the migration of the thalweg, with b as the exponent. According to Qian's research (1987), the cumulative distance of thalweg migration is directly proportional to the wandering exponent during a flood peak process. Through establishing the inverse relationship between the migration distances and the restricting indicators in all previously measured times of thalweg migration, the exponents of a and b, respectively, represent the migration items, and the boundary items can be determined. Taking into account the fact that the barrier properties can reflect the capacity and stability of the channel boundary to restrict the migration of the main stream line, the river barrier exponent can be expressed as follows:

$$\Psi = \left[\left(\frac{B}{B_{\max}}\right)^{0.6} \cdot \left(\frac{h}{B}\right)^{0.05} \cdot \left(\frac{d_{50}}{hJ}\right)^{0.1}\right]^{b}. \quad (2)$$

According to the above ideas, a method framework of this study was developed, as shown in Fig. 6.

4.2 Data

According to historical and recent aerial remote sensing images downloaded from the website of the U.S. Geological Survey (USGS), the plane morphology and the nodal location distribution of 27 typical single-thread river reaches in the MRYR were analyzed. The average daily flow and sediment concentration data for the Jianli, Luoshan, and Hankou hydrological stations in the MRYR were from the Hydrology Bureau of the Yangtze River Water Conservancy Commission, as well as the bed material composition and median particle diameter data. The planar diagrams of the thalweg migration and channel adjustment were from the Channel Planning & Design and Research Institute of the Yangtze River. The cross-sectional topographic data of typical river reaches during 1996, 1998, and 2001 were obtained from Wuhan University. The actual lengths of the nodes protruding from the river bank were measured according to the 1:10,000 topographic map in 2013. It is worth noting that 1998 represents the flood years and 2001 the dry years during the period of 1955–2013. Given the riverbed erosion in the flood years typically scaled a full cross-section, yet the scouring in the dry years usually concentrated in the deep groove, the bankfull river widths of the ‘0 m’ line in 1998 and 2001 could be considered as the minimum and maximum values of the variation ranges. Similarly, compared with the descending values of water level in these years, the scouring depths between each year could also be the extreme values of the domain.

4.2.1 Upstream river regime adjustment and nodal deflecting flow conditions

As noted above, the upstream river regime adjustment provides an initial disturbance, whose intensity can be characterized by the thalweg displacement at the entrance of the downstream reach, which can be obtained from the previous measured diagrams of thalweg migration. Because the node narrows the channel width, along the flow-path, the width to depth ratio of each cross-section decrease at first, and then increase; consequently, the node can control the upstream incoming flows from all directions and then amplify the differences of the flow directions or flow level at the outflow of the node, as shown in Fig. 7. It can be seen that the incoming flow levels and directions and the transverse constrictive degree

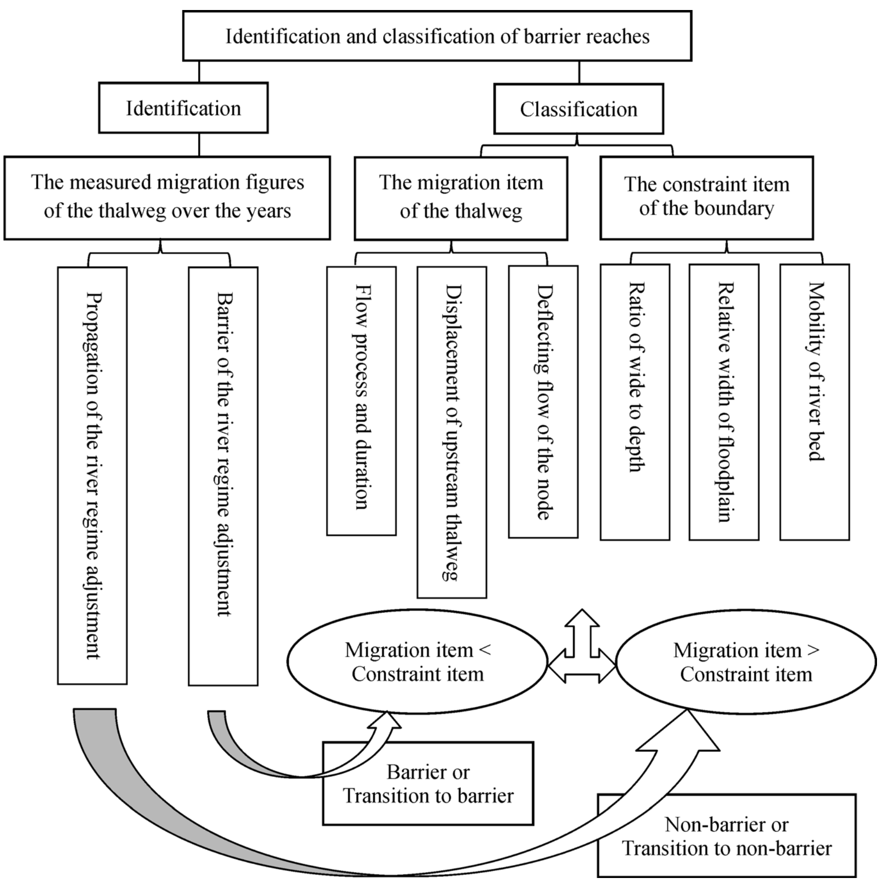

Fig. 6 The method framework of this research.

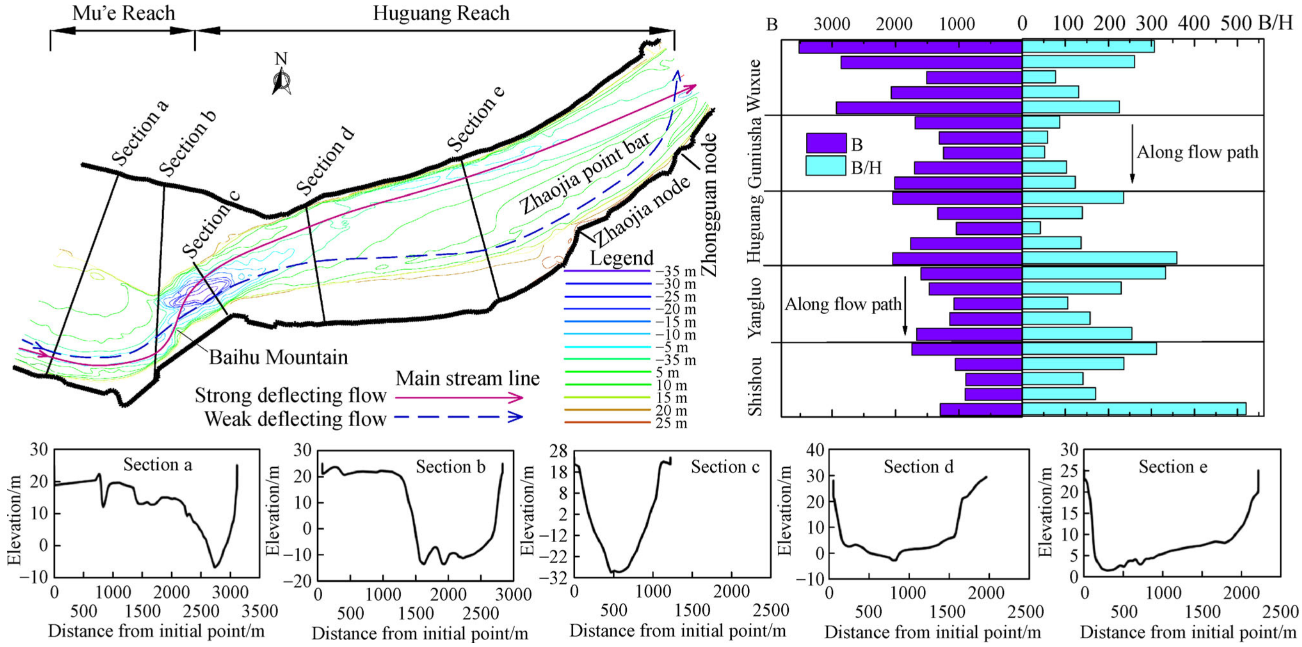

Fig. 7 Analysis graphics of the node deflecting flow.

of the node are key factors that determine the node deflecting flow strength.

4.2.2 Width–depth conditions

Although it was difficult to obtain a series of measured topographic data from 1955 to 2013, the years with the actual thalweg measurements usually had corresponding river regime adjustment charts, which contained the contours line with equal elevations to the channel navigation base level (referred to herein as the '0 m' line). As a result, the width of the '0 m' line of the typical cross-sections of each reach could be measured for each thalweg measurement time. Considering the fact that the slope ratio of the river bank was generally uniform, the correlation between the bankfull river width and the width of the '0 m' line was established according to the measured topographic data in 1996, 1998, and 2001. The relationship of Shashi–Chenglingji Reach was shown in Fig. 8(c), the relationship of Chenglingji–Wuhan Reach was shown in Fig. 8(e) and relationship of Wuhan–Hukou Reach was shown in Fig. 8(g). According to the fitting formula of the correlation relationship, the bankfull river width of each thalweg measurement was calculated according to the width of the '0 m' line.

The riverbed scour depths under bankfull water levels were estimated by considering the proportion of the descending range of the water level to the scour depth of the riverbed in the same cross-section (Fig. 8(a)). Using the field topographic data from 1996, 1998, and 2001, the value of the elevation change from 1996 to 1998, and the value from 1998 to 2000 can all be abtained. Thus, under the bankfull discharge conditions in the same year, the relationship between the descending value of the water level of the hydrological station and the scouring depth of the investigated river reach was established. Using the fitting formula to calculate the relationship between the water level and discharge in each year from 1955–2013 (Fig. 8(b)), the descending water level values under the bankfull discharge level were compared with that in 2002. Subsequently, using the same fitting formula, the scour depth of the bankfull riverbed of each measured year was obtained. Finally, according to the riverbed elevation of each measured year, which was anti-deduced from the riverbed elevation in 2002, the ratio of width to depth under the bankfull discharge condition of each measured year was calculated. The change relationship between the descending value of water level and the average value of riverbed scour depth of Shashi–Chenglingji Reach is shown in Fig. 8(d), the relationship of Chenglingji–Wuhan Reach is shown in Fig. 8(f), the relationship of Wuhan–Hukou Reach is shown in Fig. 8(h).

4.2.3 Relative width of floodplain conditions

A river reach with an unconfined river bank usually contributes to the restoration of the floodplain after a flood (Kidová et al., 2016), such as in the Medway River in Canada (Thayer and Ashmore, 2016), where the erosion resistance is poor and the floodplain is basically unrestricted, thus resulting in the accustomed migration of the main channel. However, the Downstream Tongariro River in New Zealand (Reid and Brierley, 2015), where the upstream river reaches are restricted by terraces on both

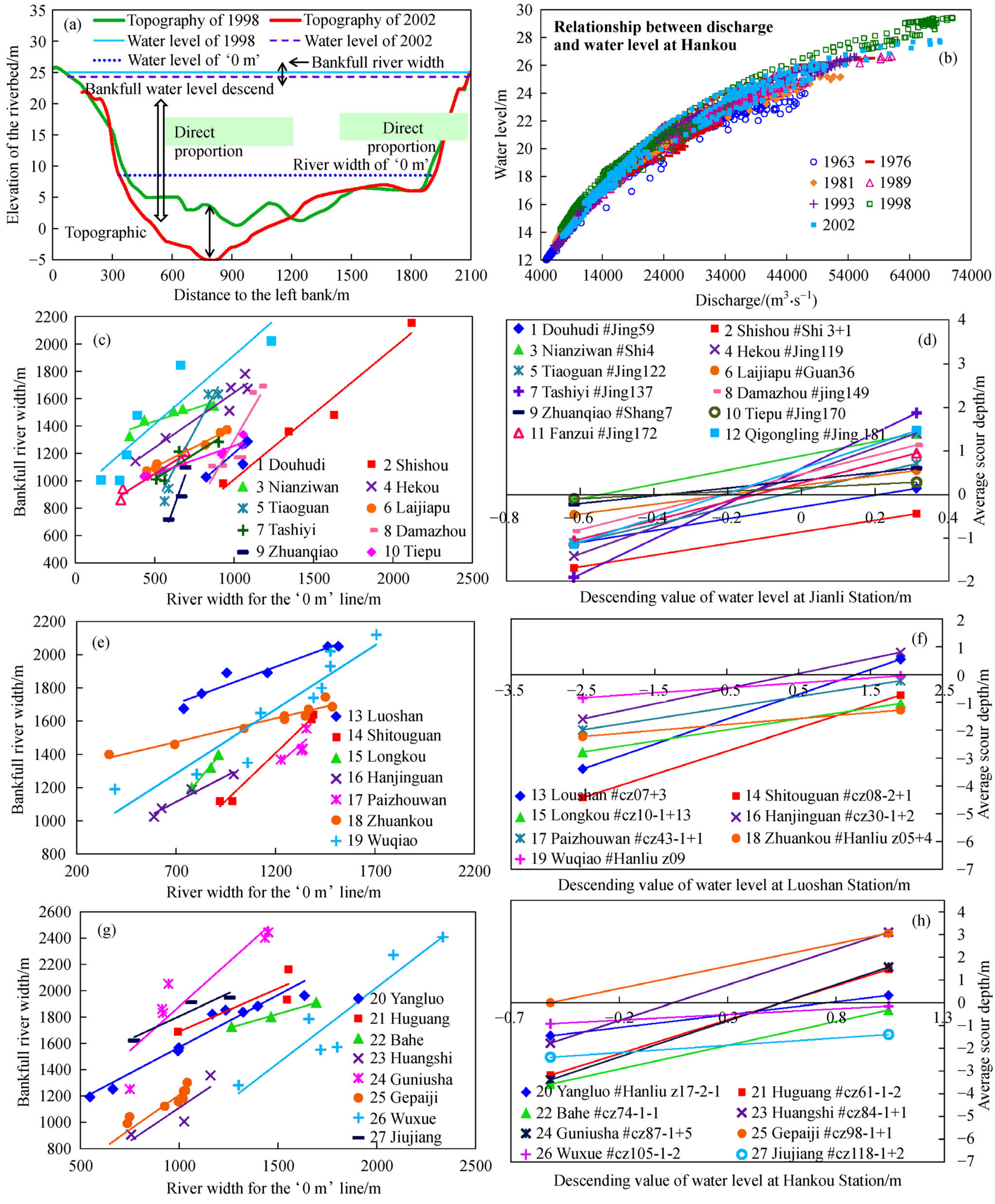

Fig. 8 Calculation diagram of the ratio of river width to depth in each measured year. (a) Calculation frame diagram of relationship between the bankfull river width and the river width of '0 m' line, relationship the riverbed scour depth and the descending value of water level; (b) Relationship between the discharge and the water level at Hankou Station; (c) Relationship between the bankfull river width and the river width of '0 m' line of Shashi–Chenglingji Reach; (d) Relationship between the riverbed scour depth and the descending value of water level of Shashi–Chenglingji Reach; (e) Relationship between the bankfull river width and the river width of '0 m' line of Chenglingji–Wuhan Reach; (f) Relationship between the riverbed scour depth and the descending value of water level of Chenglingji–Wuhan Reach; (g) Relationship between the bankfull river width and the river width of '0 m' line of Wuhan–Hukou Reach; (h) Relationship between the riverbed scour depth and the descending value of water level of Wuhan–Hukou Reach.

sides, has no floodplain. The main channel is narrow and deep where the main stream line is basically unchanged, making a barrier effect in the downstream propagation of the upstream river regime adjustment. The river width of the MRYR has been restricted by embankments and has experienced little change, thus the distances between both sides of the embankments can be treated as the widest river widths.

4.2.4 Shields number conditions

The particle size has a significant influence on the lateral migration of the thalweg (Wohl, 2015). Larger values for the medium diameter sized the bed material are associated with smaller values for the channel longitudinal gradient and larger reciprocals of the Shields number. In these cases, the friction force of the sediment resisting movement is larger than the drag force of the water flow acting on the sediment (Frings et al., 2014), resulting in an increase in the migration resistance of the thalweg and a decrease in the riverbed deformation due to the change of flow. This is beneficial for shaping a stable and contractive riverbed (Kidová et al., 2016). Conversely, smaller values for the medium diameter sized bed material are associated with smaller reciprocals of the Shields number. In these cases, there is a weaker lateral migration resistance of the thalweg (Sun et al., 2015), which is conducive to riverbed deformation. When the upstream river regime adjusts, this reach is bound to propagate the adjustments to the downstream reaches, and thus, barrier properties will be virtually nonexistent.

With increased water levels due to overflows in the floodplain, the suspended sediment carried in the water gradually deposits due to the descending flow velocity, resulting in a reduction in the cross-sectional averaged particle size of bed material. In addition, the thalweg diversions largely depend on the particle size of the floodplain. Therefore, the medium diameter and the concentration of the suspended sediment at the hydrological station influence the material composition on the floodplain and the possibility of thalweg migration. A correlation between the suspended sediment concentrations at the stations of Jianli, Luoshan, and Hankou and the medium-sized diameters of bed sediments were established (Fig. 9). Based on the above mentioned empirical results, the medium-sized diameter of bed sediment in each reach can be obtained by using the measured suspended sediment concentration over the years. The results showed that the channel longitudinal gradient was inversely proportional to the flow rate, and was proportional to the sediment concentration and the medium-sized diameter of the bed sediment. Considering that the channel longitudinal gradients were different in different river reaches, they were calculated by using the empirical relationship established by Li and Yao (1965) according to the field

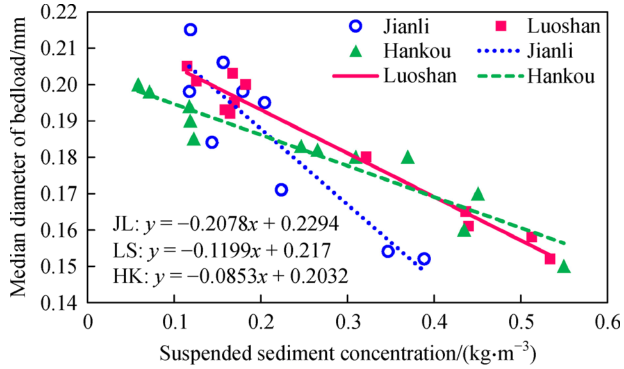

Fig. 9 Relationship between the suspended sediment concentration and the medium-sized diameter of bed sediment.

data in observed years:

$$J = 0.00455[(S/Q)^{1/2}D_{50}]^{0.59}. \tag{3}$$

Here, J is the channel longitudinal gradient (‰), Q is the bankfull discharge (m^3/s), S is the suspended sediment concentration (kg/m^3) at bankfull water level, and D_{50} is the medium diameter of bed sediment (mm).

5 Results

The riverbed evolution data of 27 single-thread river reaches in the MRYR were systematically studied. Two to three typical sections have been chosen as subjects for investigation in each river reach. Their section numbers and measured years are shown in Table 1. Based on the observed plane diagrams of the thalweg migration, the migration distance during these times could be measured and calculated. According to the calculation method in Sections 4.1 and 4.2, the restricting indicator of the thalweg migration was calculated. According to the value of the two base numbers in Eq. (1), the subregion of each river reach could be preliminarily judged. The index a, b could then be adjusted continually to determine the inversely-proportional relationship between the restricting indicators of thalweg migration and the corresponding migration distance. At this point, the adjustment directions of ‘a’ and ‘b’ were unique, and the values were always within a reasonable range, until the inversely-proportional relationship was completely built. Eventually, the index a,b could be confirmed (Table 1).

As shown in Fig. 10 and Table 1, in the Shashi–Chenglingji Reach, the relative distances of thalweg migration (the thalweg migration distance divided by the bankfull river width) of the Tiepu, Damazhou, and Nianziwan Reaches were the largest. The average thalweg migration index was as high as 0.96, but the average boundary constraint index was as low as 0.60. These findings indicate that the migration effect of the main

Table 1 The migration and constraint indexes of the single-thread reaches in the MRYR

No.	Reach name	Reach length/km	Distance from Yichang/km	Typical cross-section	Measurement year of the thalweg	Migration index	Constraint index	Barrier or not
1	Douhudi	9.9	175	Jing59, Jing61, Jing63	1970,1975,1980	0.87	1.00	Yes
2	Shishou	8	234	Shi3 + 1, Jing95	1983,1991,1996,1997,1998,2003,2004, 2005,2006	0.95	0.72	No
3	Nianziwan	15	242	Jing106, Shi4, Jing108	1999,2000,2005,2006,2007	0.92	0.66	No
4	Hekou	7	257	Jing111,Jing119	1973,1981,1995,1998,2002,2004,2006, 2008,2009	0.88	0.79	No
5	Tiaoguan	13	264	Shi6,Jing122	1973,1981,1995,1998,2002,2004,2006, 2008,2009	0.87	0.93	Yes
6	Laijiapu	12	277	Shi8,Guan39	1973,1981,1995,1998,2002,2004,2006, 2008,2009	0.87	0.85	No
7	Tashiyi	14	289	Jing135, Jing137, Jing139	1980,1987,1993,1998,2002,2004,2006, 2008	0.87	0.97	Yes
8	Damazhou	11	330	Jing147, Jing148, Jing149	1980,1987,1993,1998,2002,2004,2006, 2008	1.00	0.50	No
9	Zhuanqiao	9	338	Shang7, Li3	1980,1987,1993,1998,2002,2004,2006, 2008	0.84	0.91	Yes
10	Tiepu	12	347	Li4, Jing170, Jing171	1980,1987,1993,1998,2002,2004,2006, 2008	0.96	0.59	No
11	Fanzui	6.5	356	Jing172, Jing173	1980,1987,1993,1998,2002,2004,2006, 2008	0.84	0.89	Yes
12	Qigongling	7.8	380	Jing180, Li7, Jing181	1980,1987,1993,1998,2002,2004,2006, 2008	0.89	0.80	No
13	Luoshan	11	419	cz06-1, luoshanzx6 + 1,cz07 + 3	1972,1977,1980,1984,1992,1997,2001, 2003	1.00	0.52	No
14	Shitouguan	9	456	cz08 + 2, cz08-2 + 1	1995,1998,2000,2003,2005,2007,2008	0.92	0.81	No
15	Longkou	9.6	483	cz10-1 + 1,cz17 + 2,cz18 + 2	1959,1973,1985,1996	0.86	0.96	Yes
16	Hanjinguan	11	519	cz30-1 + 2,cz31 + 2	1977,1981,1986,1993,1996,2011	0.86	1.00	Yes
17	Paizhouwan	15	542	cz43-1 + 1,cz44 + 4	1977,1981,1986,1993,1996,2011	0.90	0.86	No
18	Zhuankou	12	610	hanliuz05 + 4, cz54-1 + 4, cz55-1 + 3	1981,1986,1993,1996,1998,2001,2006	0.93	0.72	No
19	Wuqiao	7	628	hanliuz07 + 4,hanliuz09,cz56	1981,1986,1993,1996,1998,2001,2006	0.94	0.63	No
20	Yangluo	15	658	hanliuz17-0 + 2,hanliuz17-2-1, cz57-1-2	1981,1986,1993,1996,1998,2001,2006	0.88	0.89	No
21	Huguang	10	679	cz60-1-3,cz60-2-1,cz61-1-2	1980,1992,2000,2003,2004,2005	0.95	0.66	No
22	Bahe	9.4	723	cz74-1-1,cz74-1 + 1,cz75-1	1963,1977,1980,1992,1995	0.98	0.56	No
23	Huangshi	20	753	cz83-1-1,cz84-1 + 1,cz86-1-1	1976,1980,1987,1992,2000,2003	0.87	0.94	Yes
24	Guniusha	17	773	cz87,cz87-1 + 1,cz87-1 + 5	1976,1980,1987,1992,2000,2003	0.93	0.70	
25	Gepaiji	14	802	cz96-1 + 1,cz98-1 + 1,cz100-1-1	1998,2001,2008,2011	0.87	0.98	Yes
26	Wuxue	14	830	cz105-1-2,cz106-1-1,cz107-1-2	1997,1999,2001,2002	1.00	0.50	No
27	Jiujiang	22	853	cz118-1 + 2,cz119-1 + 1, cz119-1-2	1980,1984,1986,1989,1996	0.91	0.79	No

stream was dominant, and the channel boundary conditions made it difficult to effectively restrict the main stream migration; thus, these reaches were classified as non-barrier river reaches. The relative distances of the thalweg migration for the Hekou, Qigongling, Shishou, and Laijiapu Reaches were the second largest in terms of rank, and the average migration index was 0.88, while the average constraint index was 0.77. These findings indicate that the main stream migration effect was still dominant, but the channel boundary conditions were strengthened. When the upstream river regime or incoming flow condition changes advantageously, the migrating condition

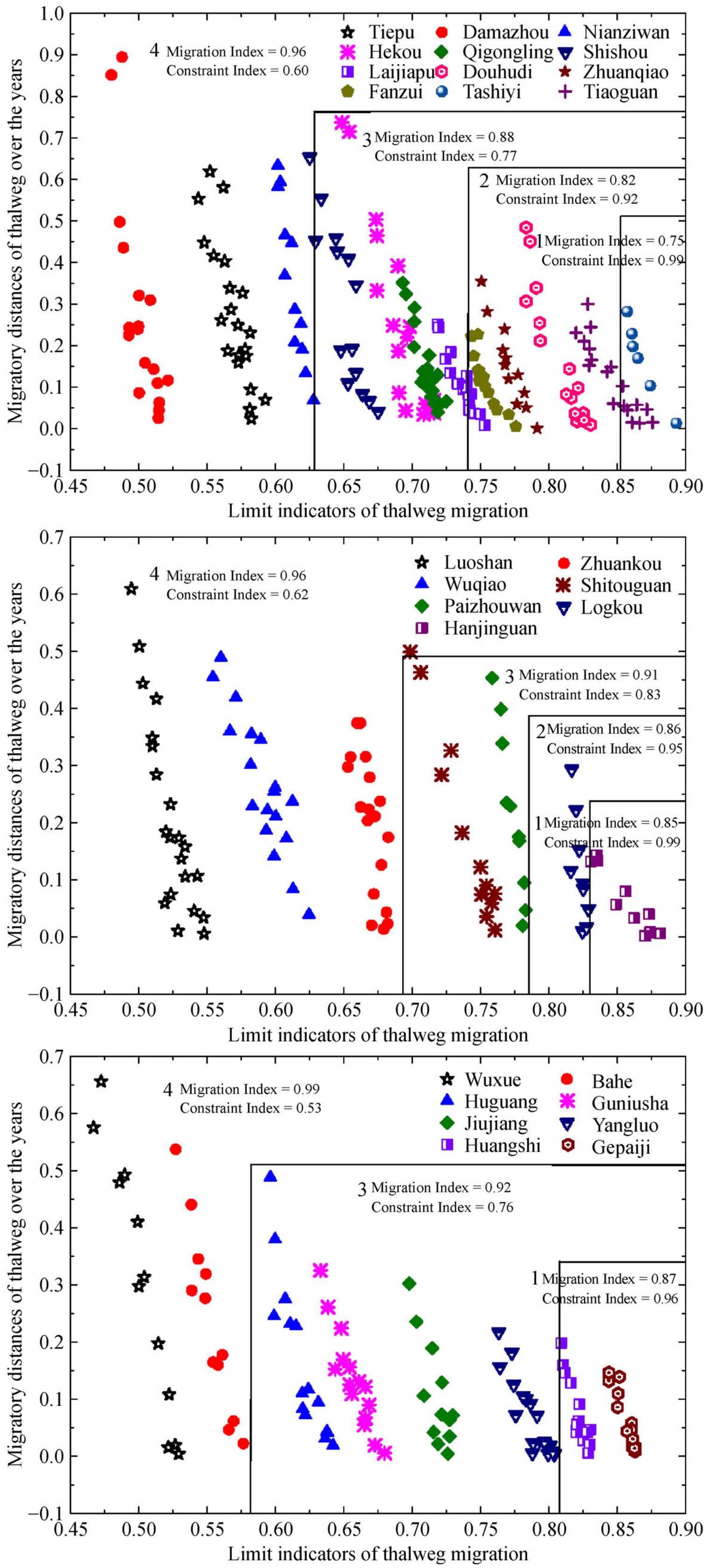

Fig. 10 The division of the barrier degree for single-thread river reaches. District 1 = barrier reaches; District 2 = transitional reaches transforming from barrier to non-barrier; District 3 = transitional reaches transforming from non-barrier to barrier; District 4 = non-barrier reaches.

will weaken. These reaches may maintain the stability of the main stream position to a certain extent; hence, they were deemed as transitional river reaches transforming from non-barriers to barriers. The average migration index of the Douhudi, Tiaoguan, Zhuanqiao, and Fanzui Reaches was 0.82, and the average constraint index was 0.92, thus the restraint effect of the boundary conditions was further enhanced. However, when the upstream river regime or incoming flow condition was adversely affected, reinforcing the migration, the boundary conditions were unable to maintain main stream line stability, and thus were deemed as transitional river reaches transformed from barriers to non-barriers. In the Tashiyi Reaches, the average migration index was 0.75 and the average constraint index was 0.99. These findings indicate that the restraint effect of the channel boundary was dominant, and even if the migrating condition was strengthened, the channel boundary conditions may still maintain the stability of the main stream line. Thus, these reaches were classified as the barrier river reaches.

In the Chenglingji–Wuhan Reach, the average migration index of the Luoshan, Zhuankou, and Wuqiao Reaches was as high as 0.96, but the average constraint index was only 0.62. These reaches represent non-barrier river reaches. The average migration index of the Shitouguan, Paizhouwan Reach was 0.91, while the average constraint index was 0.83. Thus they were classified as transitional river reaches transforming from non-barrier to barrier. The migration index of Longkou was 0.86, while the constraint index was 0.95; hence, this reach represented a transitional river reach transforming from barrier to non-barrier. Lastly, the migration index of Hanjinguan was 0.85, while the constraint index was 0.99; thus representing a barrier river reach. In the Wuhan–Hukou Reach, the average migration index of the Wuxue and Bahe Reaches was as high as 0.99, but the average constraint index was only 0.53, thus classified as non-barrier river reaches. The average migration index of the Huguang, Guniusha, Jiujiang, and Yangluo Reaches was 0.92, while the average constraint index was 0.76, and thus they were classified as transitional river reaches transforming from non-barrier to barrier. The average migration index of Huguang and Gepaiji Reach was 0.87, while the average constraint index was 0.96, with a classification of barrier river reaches.

So far, the barrier properties of the 27 single-thread river reaches in the middle reaches of the Yangtze River have been divided into four categories, as shown in Fig. 11. In the process of river management, the protection and maintenance of existing barrier properties should be prioritized given their effectives in stabilizing the river regime when compared to artificial river regulations. Conversely, transformation from non-barrier to barrier reaches should be supported to create more of a barrier effect, which is conducive to the stability of the downstream reaches.

6 Conclusions

Upstream river regime adjustments are one of the main influencing factors for downstream channel evolution. However, not all river regime adjustments will propagate downstream. There are some special river reaches where upstream and downstream river regime adjustments are not relevant. This non-correlation is neither due to the different water and sediment conditions nor to different river types, but instead is driven by an in-between barrier river reach itself blocking the flow-topography dynamic connectivity

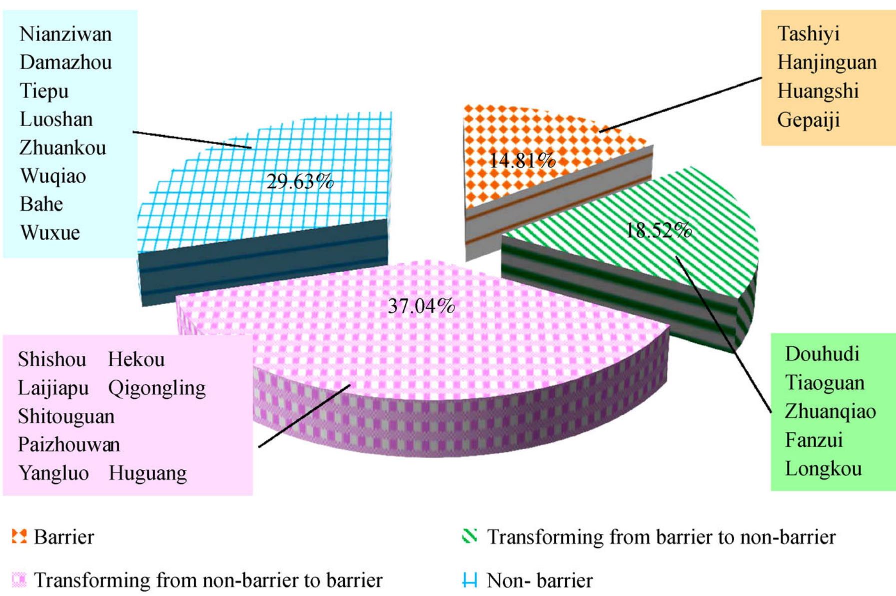

Fig. 11 Classification for the barrier degree of single-thread river reaches in the MRYR.

between the upstream and downstream reaches. This study shows that as long as there is no artificial disturbance to destroy the boundary condition of the barrier river reach, due to its strong anti-erosion boundary, it can maintain its own cross-sectional equilibrium of sediment transport no matter the flow and sediment condition changes or the upstream river regime adjustments. It will also sustain the position and direction of the thalweg line and maintain the riverbed morphology. Thus, a barrier river reach will prevent the upstream river regime adjustments from affecting the downstream channel evolution, eventually blocking the propagating effect of the river regime adjustments.

The migration of the main stream line or the thalweg line is the main way by which the upstream river regime adjustment can propagate downstream. Based on a systematic summary of the evolution regularities of the MRYR, the influencing factors of the thalweg migration were extracted and analyzed. These factors included the ratio of the average flow above the critical bankfull discharge to the average flow below the critical bankfull discharge, the ratio of the duration days of the aforementioned two periods, the displacement of the thalweg at the entrance of the river reach, the deflecting flow intensity of the node, the ratio of the river width to water depth, the relative width of the floodplain, and the Shields number. Through establishing empirical relationships between the observed thalweg migration distance and the synchronous restricting indicator of the thalweg migration over the years, the barrier degree of 27 single-thread river reaches in the MRYR was assessed. This analysis revealed 4 barrier river reaches (with a migrating index much larger than the constraint index); 5 transitional river reaches transforming from barriers to non-barriers (with boundary conditions making it difficult to restrict the main stream line migration once the migration condition of the incoming flow was enhanced, even though its constraint index was larger); 10 transitional river reaches transforming from non-barriers to barriers (where the boundary may maintain main stream line stability when the migrating condition is weaker, even though its constraint index is smaller); and 8 non-barrier river reaches (with a migration index far less than the constraint index).

Acknowledgements This research was supported by Open Research Fund of CRSRI (No. CKWV2018464/KY), the National Key Research and Development Program of China (Nos. 2016YFC0402306, 2016YFC0402310, and 2016YFC0402106), Key Program of the National Natural Science Foundation of China (Grant No. 51379155), and Fundamental Research Funds for Central Welfare Research Institutes (No. TKS160103).

References

Armaş I, Gogoaşe Nistoran D E, Osaci-Costache G, Braşoveanu L (2013). Morpho-dynamic evolution patterns of Subcarpathian Prahova River (Romania). Catena, 100(2): 83–99

Campana D, Marchese E, Theule J I, Comiti F (2014). Channel degradation and restoration of an alpine river and related morphological changes. Geomorphology, 221(11): 230–241

Chen J, Wang Z, Li M, Wei T, Chen Z (2012). Bedform characteristics during falling flood stage and morphodynamic interpretation of the middle–lower Changjiang (Yangtze) River channel, China. Geomorphology, 147–148: 18–26

Cserkész-NagyÁ, Tóth T, Vajk Ö, Sztanó O (2010). Erosional scours and meander development in response to river engineering: middle Tisza region, Hungary. Proceedings of the Geologists' Association, 121(2): 238–247

David M, Labenne A, Carozza J M, Valette P (2016). Evolutionary trajectory of channel planforms in the middle Garonne River (Toulouse, SW France) over a 130-year period: contribution of mixed multiple factor analysis (MFAmix). Geomorphology, 258: 21–39

Davis W M (1899). The geographical cycle. The Geographical Journal. Washington, 14(5): 481

Downs P W, Gregory K J (1993). The sensitivity of river channels in the landscape system. In: Thomas D S G, Allison R J, eds. Landscape Sensitivity. Chichester: Wiley, 15–30

Ferguson R I (1981). Channel form and channel changes. In: Lewin J, ed. British River. Longdon: Allen and Unwin, 90–211

Frings R M, Döring R, Beckhausen C, Schüttrumpf H, Vollmer S (2014). Fluvial sediment budget of a modern, restrained river: the lower reach of the Rhine in Germany. Catena, 122(12): 91–102

Fryirs K A, Brierley G J, Preston N J, Spencer J (2007). Catchment-scale (dis)connectivity in sediment flux in the upper Hunter catchment, New South Wales, Australia. Geomorphology, 84(3–4): 297–316

Gilbert G K, Dutton C E (1877). Report on the geology of the Henry Mountains. Geographical and Geological Survey of the Rocky Mountain Region (U.S.)

Goodbred S L Jr, Kuehl S A (1998). Floodplain processes in the Bengal Basin and the storage of Ganges—Brahmaputra river sediment: an accretion study using ^{137}Cs and ^{210}Pb geochronology. Sediment Geol, 121(3–4): 239–258

Hack J T (1960). Interpretation of erosional topography in humid temperate regions. American Journal of Science, 258-A: 80–97

Hajdukiewicz H, Wyżga B, Mikuś P, Zawiejska J, Radecki-Pawlik A (2016). Impact of a large flood on mountain river habitats, channel morphology, and valley infrastructure. Geomorphology, 272: 55–67

Han Q W (2011). Equilibrium trend of sediment transportation and river morphology. J Sediment Res, 8(4): 1–14 (in Chinese)

Henshaw A J, Gurnell A M, Bertoldi W, Drake N A (2013). An assessment of the degree to which Landsat TM data can support the assessment of fluvial dynamics, as revealed by changes in vegetation extent and channel position, along a large river. Geomorphology, 202: 74–85

Huang X Q, Liu Z J (1991). A study on the inner structure and spatial effect of the braided pattern in the lower reaches of the Chang Jiang (Yangzi River). Acta Geographica Sinica, (2): 169–177 (in Chinese)

Jun Q, Yang Z F, Shen Z Y (2012). Three-dimensional modeling of sediment transport in the Wuhan catchments of the Yangtze River. Procedia Environ Sci, 13: 2437–2444

Kidová A, Lehotská M, Rusnák M (2016). Geomorphic diversity in the braided-wandering Belá River, Slovak Carpathians, as a response to flood variability and environmental changes. Geomorphology, 272: 137–149

Leopold L B, Wolman M G (1957). River channel patterns- braided, meandering, and straight. The Professional Geographer, 9: 39–85

Li B R, Yao Y L (1965). Calculation method of longitudinal gradient and longitudinal profile. Yellow River, 4: 32–36 (in Chinese)

Lobera G, Besné P, Vericat D, López-Tarazón J A, Tena A, Aristi I, Díez J R, Ibisate A, Larrañaga A, Elosegi A, Batalla R J (2015). Geomorphic status of regulated rivers in the Iberian Peninsula. Sci Total Environ, 508(508C): 101–114

Nanson G C, Croke J C (1992). A genetic classification of floodplains. Geomorphology, 4(6): 459–486

Nanson R A, Nanson G C, Huang H Q (2010). The hydraulic geometry of narrow and deep channels; evidence for flow optimisation and controlled peatland growth. Geomorphology, 117(1–2): 143–154

Qian N, Zhang R, Zhou Z D (1987). Fluvial Process. Beijing: Science Press (in Chinese)

Ramos J, Gracia J (2012). Spatial-temporal fluvial morphology analysis in the Quelite river: it's impact on communication systems. J Hydrol (Amst), 412–413: 269–278

Reid H E, Brierley G J (2015). Assessing geomorphic sensitivity in relation to river capacity for adjustment. Geomorphology, 251: 108–121

Roy S, Sahu A S (2015). Quaternary tectonic control on channel morphology over sedimentary low land: a case study in the Ajay-Damodar interfluve of Eastern India. Geoscience Frontiers, 6(6): 927–946

Rust B R (1977). A classification of alluvial channel systems. Dallas Geological Society, 1977: 187–198

Schumm S A (1985). Patterns of alluvial rivers. Annual Review of Earth and Planetary Sciences, 13(1): 5–27

Schumm S A, Khan H R (1971). Experimental Study of Channel Patterns. Nature, 233(5319): 407–409

Schuurman F, Kleinhans M G, Middelkoop H (2016a). Network response to disturbances in large sand-bed braided rivers. Earth Surface Dynamics, 4(1): 25–45

Schuurman F, Shimizu Y, Iwasaki T, Kleinhans M G (2016b). Dynamic meandering in response to upstream perturbations and floodplain formation. Geomorphology, 253: 94–109

Song X L, Xu G Q, Bai Y C, Xu D (2016). Experiments on the short-term development of sine-generated meandering rivers. Journal of Hydro-environment Research, 11: 42–58

Sun J, Lin B L, Yang H Y (2015). Development and application of a braided river model with non-uniform sediment transport. Advances in Water Resources, 81(45): 62–74

Thayer J B, Ashmore P (2016). Floodplain morphology, sedimentology, and development processes of a partially alluvial channel. Geomorphology, 269: 160–174

van Dijk W M, Schuurman F, van de Lageweg W I, Kleinhans M G (2014). Bifurcation instability and chute cutoff development in meandering gravel-bed rivers. Geomorphology, 213: 277–291

van Dijk W M, van de Lageweg W I, Kleinhans M G (2013). Formation of a cohesive floodplain in a dynamic experimental meandering river. Earth Surface Processes and Landforms, 38(13): 1550–1565

Wang S J (2003). Architectures, relationships between discharges and width/depth ratios of stream cross profiles, and stream powers of anastomosing rivers. Acta Sedimentologica Sinica, 21(4): 565–564 (in Chinese)

Wang S J, Yin S P (2000). Discussion on channel patterns of anastomosing and anabranched rivers. Earthence Frontiers, (b08): 79–86 (in Chinese)

Wohl E (2015). Particle dynamics: the continuum of bedrock to alluvial river segments. Geomorphology, 241: 192–208

Wolman M G, Gerson R (1978). Relative scales of time and effectiveness of climate in watershed geomorphology. Earth Surface Processes, 3(2): 189–208

Xia J Q, Deng S S, Lu J Y, Xu Q X, Zong Q L, Tan G M (2016). Dynamic channel adjustments in the Jingjiang Reach of the Middle Yangtze River. Scientific Reports, 6(1): 1–10

Xia J Q, Zong Q L, Deng S S, Xu Q X, Lu J Y (2014). Seasonal variations in composite riverbank stability in the Lower Jingjiang Reach, China. Journal of Hydrology, 519: 3664–3673

Xu D, Bai Y C(2013). Experimental study on the bed opography evolution in alluvial meandering rivers with various sinuousnesses. Journal of Hydro-environment Research, 7(2): 92–102

You X Y, Tang J W (2017b). Phenomena and characteristics of barrier river reaches in the middle and lower Yangtze River, China. Journal of Earth System Science, 126(4): 61

You X Y, Tang J W, Zhang X F, Hou W G, Yang Y P, Sun Z H, Weng Z H, (2017a). The mechanism of barrier river reaches in the middle and lower Yangtze River. Journal of Geographical Sciences, 27(10): 1249–1267

You X Y, Tang J W, Zhang X F, Li Y T (2016). Preliminary study on the characteristics and origin of barrier river reach in the Middle and Lower Yangtze River. Journal of Hydraulic Engineering, 47(4): 545–551

Zhang W, Yang Y P, Zhang M J, Li Y T, Zhu L L, You X Y, Wang D, Xu J F, (2017). Mechanisms of suspended sediment restoration and bed level compensation in downstream reaches of the Three Gorges Projects (TGP). Journal of Geographical Sciences, 27(4): 463–480

Zolezzi G, Güneralp I (2016). Continuous wavelet characterization of the wavelengths and regularity of meandering rivers. Geomorphology, 252(3): 98–111